Geomechanics and Engineering, *Vol. 28, No. 1 (2022) 77-87*
https://doi.org/10.12989/gae.2022.28.1.077

Stability analyses of dual porosity soil slope

Alfrendo Satyanaga[a], Sung-Woo Moon[b] and Jong R. Kim*

Department of Civil and Environmental Engineering, Nazarbayev University, Nur-Sultan 010000, Kazakhstan

(Received April 26, 2021, Revised October 22, 2021, Accepted November 2, 2021)

Abstract. Many geotechnical analyses require the investigation of water flow within partially saturated soil zone to incorporate the effect of climatic conditions. It is widely understood that the hydraulic properties of the partially saturated soil should be included in the transient seepage analyses. However, the characteristics of dual porosity soils with dual-mode water retention curve are normally modelled using single-mode mathematical equation for simplification of the analysis. In reality, the rainwater flow can be affected significantly by the dual-mode hydraulic properties of the soil. This paper presents the variations of safety factor for dual porosity soil slope with dual-mode water retention curve and dual-mode unsaturated permeability. This paper includes the development of the new dual-mode unsaturated permeability to represent the characteristics of soil with the dual-mode water retention curve. The finite element analyses were conducted to examine the role of dual-mode water retention curve and dual-mode unsaturated permeability on the variations of safety factor under rainfall loading. The results indicate that the safety factor variations of dual porosity soil slope modelled using the dual-mode water retention curve and the unsaturated permeability equation are lower than those of dual porosity slope modelled using single-mode water retention curve and unsaturated permeability equations.

Keywords: numerical analyses; safety factor; seepage; slope stability; partially saturated soil

1. Introduction

Tropical areas with abundant of rainfall and prolonged dry period are normally associated with rainfall-induced landslides (Kristo *et al.* 2019, Satyanaga *et al.* 2019, Rahardjo *et al*. 2019, Qi *et al*. 2019). Studies by Rahardjo and Satyanaga (2019a), Kim and Jeong (2017), Mustafa *et al.* (2015) and Kassim *et al*. (2012) indicated that majority of the slip surfaces of slope failures from these areas are encountered within partially saturated zone. Therefore, the comprehensive transient seepage analyses are necessary in the design of slope preventive measures for assessment of the influence of rainfall loading on the slope stability under partially saturated condition. Fredlund *et al*. (2012) and Fredlund and Rahardjo (1993) observed the unsaturated hydraulic properties are very crucial influencing the rate of water flow within the partially saturated soil zone near ground surface. They also indicated that the shear strength of the partially saturated soil varies with the changes in water content and soil suction or negative pore-water pressure. This phenomenon was also observed by Rahardjo *et al.* (2009) and Deng *et al.* (2020).

The hydraulic properties of the partially saturated soil are related to water retention curve and unsaturated permeability function. Many researchers who are conducting research works on residual soils, indicate the gap-graded characteristics of some residual soils with dual-mode water retention curve and dual-mode unsaturated permeability (Zhai *et al.* 2017, 2020, Satyanaga *et al.* 2013, Satyanaga and Rahardjo 2019b). Up to date, almost all numerical analyses never incorporate the dual-mode characteristics of dual porosity soils to determine the stability of the slope. The water retention curve and the unsaturated permeability of dual porosity soil are usually modelled with mathematical equations for single-mode characteristic to avoid the complexity of the analyses. The simplification from dual-mode to single-mode model would attribute to the erroneous in the results from numerical analyses since the behavior of rainwater flow into dual-porosity soil layer is not modelled appropriately.

A lot of researchers observed that the water retention curve is analogous to the distribution of soil pores (Zhai *et al*. 2017, 2018, Zhai and Rahardjo 2015, Fredlund *et al.* 1994, Rahimi *et al*. 2015). The macro- and micro-pores of soil are commonly related to the first and second sub-curves in water retention curve, respectively. Studies by Kunze *et al.* (1968) and Childs and Collis-George (1950) indicated that the shape of water retention curve is similar to the shape of the unsaturated permeability. Therefore, the unsaturated permeability can be calculated from water retention curve according to the pore-size distribution concept. Because finite element method generally requires continuous data of the unsaturated permeability in the transient seepage analyses, majority of previous research works focused on the best fitting equation of the single-mode unsaturated permeability.

The main aim of this research work is to study the

*Corresponding author, Professor
E-mail: jong.kim@nu.edu.kz
[a]Assistant Professor
E-mail: alfrendo.satyanaga@nu.edu.kz
[b]Assistant Professor
E-mail: sung.moon@nu.edu.kz

ISSN: 2005-307X (Print), 2092-6219 (Online)

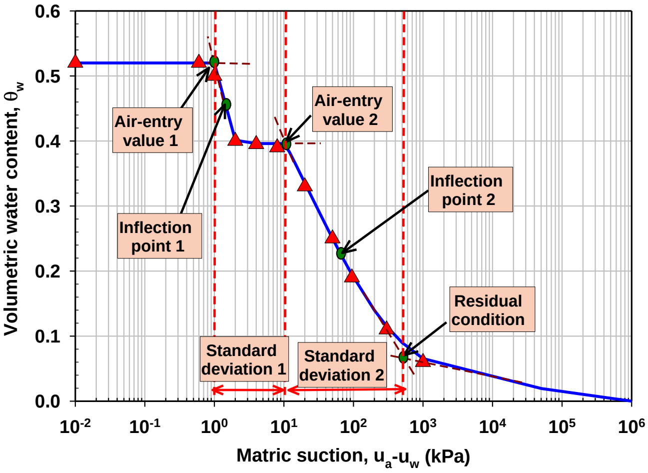

Fig. 1 Variables of dual-mode water retention curve with its variables based on Eq. (1)

stability of dual porosity soil slope which is associated with dual-mode water retention curve and dual-mode unsaturated permeability. The new mathematical equation to represent the dual-mode unsaturated permeability is proposed in this paper. The water retention curve and the unsaturated permeability of soils which were modelled with the new dual-mode equation were incorporated in the analyses to show the influence of dual-porosity soil on the stability of the slope. The results of the analyses were compared with those analyses utilizing the water retention curve and the unsaturated permeability modelled with the single-mode equation.

2. Theory and equation

2.1 Literature review

A mathematical equation is necessary for best fitting water retention curve since its continuous function provides convenience to geotechnical engineers for seepage analysis and estimation of other partially saturated properties (Fredlund *et al*. 2012). Previous researchers have proposed different equations for best fitting single-mode (Fredlund and Xing 1994, Kosugi 1994, Pedroso *et al*. 2009, Leong and Rahardjo 1997, Satyanaga *et al*. 2017) and dual-mode water retention curve (Satyanaga *et al*. 2013, Zhang and Chen 2005, Sheng 2011).

The dual-model mathematical equations for water retention curve were classified into three groups (Wijaya and Leong 2016). In the first group of equation, the merging point of two sub-curves was determined randomly and the fitting parameters of two sub-curves of water retention curve were obtained independently (Wilson *et al*. 1992, Burger and Shackelford 2001, Smettem and Kirkby 1990). In the second group of equation, the water contents of macro- and micro-pores under saturated conditions were separated and the fitting parameters of two sub-curves of water retention curve were obtained simultaneously (Mallants *et al*. 1997, Zhang and Chen 2005, Othmer *et al*. 1991, Durner 1994, Ross and Smettem 1993). In the last group of equation, the initial value of some parameters for the best fitting equation were determined graphically from the water retention curve and the best fitting parameters were obtained using the curve fitting technique (Satyanaga *et al*. 2013, Li *et al*. 2014, Gitirana and Fredlund 2004, Al-Mahbashi *et al*. 2015). In this study, equation 1 (Satyanaga *et al*. 2013) was used to best fit the water retention curve from the experimental data since the fitting parameters in this equation can be related to soil properties. The variables of dual-mode water retention are presented in Fig. 1.

$$\theta_w = \left[1 - \frac{ln\left(1+\frac{\psi}{C_r}\right)}{ln\left(1+\frac{10^6}{C_r}\right)}\right]\left[\begin{array}{l}\theta_r + \left\{(\theta_{s1}-\theta_{s2})\left(1-(\beta_1)erfc\left(\frac{ln\left(\frac{\psi_{a1}-\psi}{\psi_{a1}-\psi_{m1}}\right)}{s_1}\right)\right)\right\} \\ + \left\{(\theta_{s2}-\theta_r)\left(1-(\beta_2)erfc\left(\frac{ln\left(\frac{\psi_{a2}-\psi}{\psi_{a2}-\psi_{m2}}\right)}{s_2}\right)\right)\right\}\end{array}\right] \quad (1)$$

where:

θ_{s1} = saturated volumetric water content

θ_{s2} = volumetric water content related to air-entry value 2

β_1 = 0 when $\psi \le \psi_{a1}$; β_1 = 1 when $\psi > \psi_{a1}$

β_2 = 0 when $\psi \le \psi_{a2}$; β_2 = 1 when $\psi > \psi_{a2}$

ψ_{a1} = parameter related to air-entry value 1 (kPa) (Figure 1)

ψ_{a2} = parameter related to air-entry value 2 (kPa) (Figure 1)

C_r = input parameter according to Fredlung and Xing (1994) theory (kPa)

erfc = the complementary error function, $erfc(x) = \int_{-\infty}^{x} \frac{1}{\sqrt{2\pi}} exp\left(-\frac{x^2}{2}\right) dx$

ψ_{m1} = parameter related to suction at the inflection point 1 (Fig. 1)

ψ_{m2} = parameter related to suction at the inflection point 2 (Fig. 1)

θ_r = parameter related to volumetric water content at residual condition (Fig. 1)

s_1 = parameter related to geometric standard deviation 1 (Fig. 1)

s_2 = parameter related to geometric standard deviation 2 (Fig. 1)

The subscript 1 and 2 in the equation are associated with sub-curve 1 (macro pores) and sub-curve 2 (micro pores) of dual-porosity soils, respectively.

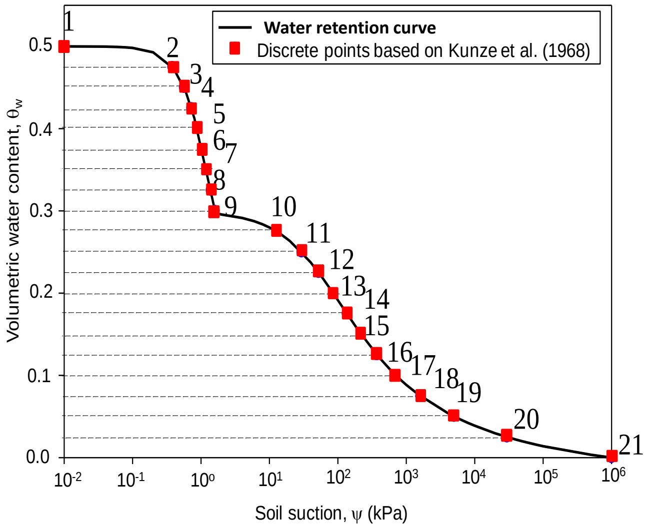

Fig. 2 Division of the water retention curve for determination of the partially saturated permeability for dual porosity soil

The determination of the unsaturated permeability is commonly carried out using indirect method based on the water retention curve and saturated permeability. Previous studies (Zhai and Rahardjo 2015, Rahimi *et al*. 2015) indicated that the statistical model is usually adopted by researchers to determine the unsaturated permeability. This model was derived based on the similarity between the water retention curve and the pore-size distribution of soil. The concept of "cutting and rejoining" is used in this model to determine the unsaturated permeability from water retention curve incorporating the probability of random connection. The determination of the unsaturated permeability based on statistical model is carried out by dividing the water retention curve equally along the volumetric water content with the same pore-size density for each division (Childs and Collis-George 1955, Krisnanto *et al*. 2020). This method was adopted to determine the unsaturated permeability of the dual-porosity soil in this study.

2.2 Proposed equation

The procedure for determination of the unsaturated permeability in this study involves dividing the water retention curve into several divisions of volumetric water content with equal increments, where $(\theta_w)_i$ and its corresponding suctions, ψ_i, can be determined for each increment. The summation of the suction values corresponding to $(\theta_w)_i$ generates the coefficient of permeability with respect to certain volumetric water content, $k(\theta_w)_i$. The accurate fit of the unsaturated permeability is provided by the matching factor $(\frac{k_s}{k_{sc}})$. The similarity of the water retention curve shape and the unsaturated permeability is provided by the terms inside the summation sign. Fredlund *et al*. (2012) indicated that the unsaturated permeability beyond residual stress state is more related to vapor flow. Therefore, the coefficient of permeability is assumed to be constant for suction larger than the residual suction. For practical reason, the unsaturated permeability is cut off at a certain small coefficient of permeability to expedite the numerical calculations. The similar method can be applied to dual-mode water retention curve (Fig. 2). As a result, the suction range between any 2 points is the same for the entire suction range of water retention curve.

Since the unsaturated permeability follows the shape of the water retention curve, the development of the proposed mathematical equation for the unsaturated permeability of dual-porosity soil was derived following lognormal distribution function. Modifying the mathematical equation for water retention curve of dual-porosity soil (Eq. (1)), it provides the new equation for modelling dual-mode permeability function as presented in equation 2. Parameter ψ_{a1} and ψ_{a2} are determined based on the air-entry value of soil associated with sub-curves 1 and 2, respectively.

$$k_w = (k_{s1} - k_{s2})\left(1 - erfc\frac{ln\left(\frac{\psi_{a1} - k_w}{k_{a1} - k_{m1}}\right)}{s_{k1}}\right) + (k_{s2})\left(1 - erfc\frac{ln\left(\frac{\psi_{a2} - k_w}{k_{a2} - k_{m2}}\right)}{s_{k2}}\right) \tag{2}$$

where:

s_k = parameter related to geometric standard deviation of permeability function

k_m = parameter associated with matric suction within inflection point

ψ_a = parameter associated with air-entry value of soil obtained from water retention curve

k_w = coefficient of permeability for different suction

ψ = designated matric suction

k_s = measured saturated permeability from laboratory testing

The terms 1 and 2 in the equation are associated with macro pores and micro pores of soil with dual-mode water

Table 1 Index properties of soils

Description	Soils				
	Soil A	Soil B	Soil C	Soil D	Soil E
USCS	CL	CL	ML	MH	SP
Gravel (%)	0	0	2.2	0	3.3
Sand (%)	35	22	31.4	40	93.5
Silt (%)	26	52	40.1	57	0.2
Clay (%)	39	26	26.3	3	3
Liquid Limit, LL (%)	54	28	42	54	NA
Plastic Limit, PL (%)	32	18	15	39	NA
Plasticity Index, PI (%)	22	10	27	15	NA
Saturated permeability, k_s (m/s)	1 x 10^{-5}	5 x 10^{-6}	5 x 10^{-5}	6 x 10^{-6}	7 x 10^{-5}

retention curve, respectively.

Eq. (2) can be simplified into Eq. (3) for best fitting soil with single-mode permeability function.

$$k_w = (k_s)\left(1 - erfc\frac{ln\left(\frac{\psi_a - k_w}{k_a - k_m}\right)}{s_k}\right) \quad (3)$$

2.3 Criteria for comparison single-mode and dual-mode equations

In this study, the accuracy in single-mode and dual-mode equations in representing the experimental data of water retention curve for dual porosity soil is assessed based on two criteria, average relative error (ARE) and Root mean squared error (RMSE). The performance of either single-mode or dual-mode equation in modelling the experimental data of water retention curve is considered good if ARE is less than 20% following study by Satyanaga *et al.* (2013). The definition of ARE is presented in Eq. (4).

$$ARE = \frac{\sum_{i=1}^{n}\left|\frac{y_{li} - y_{mi}}{y_{li}}\right|}{n} x100 \quad (4)$$

where:

n = The amount of data used in the study

y_{li} = experimental Data

y_{mi} = calculated data using the single-mode or dual-mode equation

The better capability of the mathematical model is indicated by the smaller value of RMSE. Eq. (6) presents the RMSE definition.

$$RMSE = \sqrt{\frac{\sum_{i=1}^{n}(y_{li} - y_{mi})^2}{n}} \quad (5)$$

3. Soil properties used in this study

The soil data used in this study were extracted from published literatures. The soil classification was carried out based on Unified Soil Classification System (USCS) (ASTM D2487-10, 2010; Rahardjo *et al.* 2018). The index properties of the investigated soils are presented in Table 1. Soils A, B, C, D and E were obtained from the studies in Brasil (Coutinho *et al.* 2011), Thailand (Jotisankasa *et al.* 2009), Thailand (Jotisankasa and Mairaing 2010), Singapore (Rahardjo *et al.* 2012) and Singapore (Rahardjo *et al.* 2011), respectively. Residual soil from Singapore (Soil E) has the largest percentage of sand as compared to others soils. Hence, its saturated permeability is the highest as compared to other soils.

The experimental data of water retention curve from all soils in Table 1 are presented in Figs. 3 to 5. The single-mode and dual-mode equations proposed by Satyanaga *et al.* (2013) were used to best fit the experimental data of the water retention curve from the investigated soils. Tables 2 and 3 present the variables of water retention curve from each investigated soil. The comparative studies were performed on the variables of water retention curve of the investigated soils generated from single-mode and dual-mode equations. The variables from single-mode best fitting equation indicated that soil with lower percentage of sand is associated with higher saturated volumetric water content, gentler slope (lower parameter s) and higher air-entry value (higher parameter ψ_a). The variables from dual-mode best fitting equation showed the similarity of the patterns for the air-entry value of the sub-curve 1 from the water retention curve best fitted using dual-mode equation with the air-entry value of water retention curve best fitting using single-mode equation. The trends of the air-entry value of the sub-curve 2 from the water retention curve best fitted using dual-mode equation are functions of soil particles (size and distribution) as well as soil structures (water content, density and void ratio). This observation is similar to the investigation results from Delleur (1999) and Fredlund *et al.* (2002).

The values of ARE and RMSE are presented in Figs. 3 and 4. Subscript u and b in Tables 2 and 3 represent single-mode and dual-mode soils, respectively. It can be summarized from these two tables that soils A to E have lower values of RSMEb and AREb as compared to values of RSMEu and AREu. This result indicates that the experimental data of the water retention curve follows the dual-mode characteristics and they can be classified as dual-porosity soils.

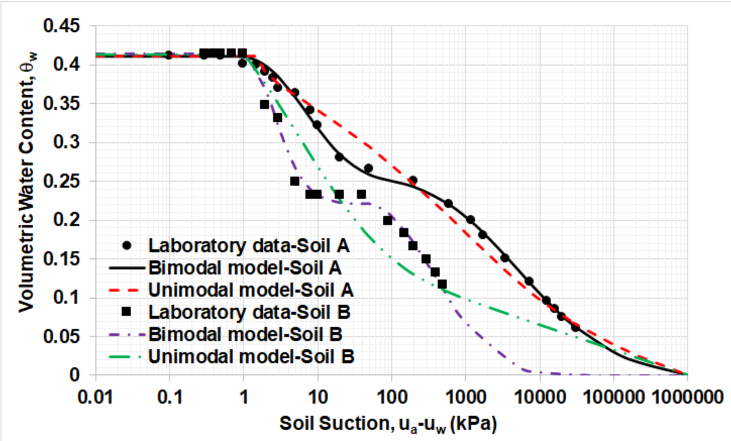

Fig. 3 Water retention curve of soils A and B modelled with dual-mode and single-mode equations

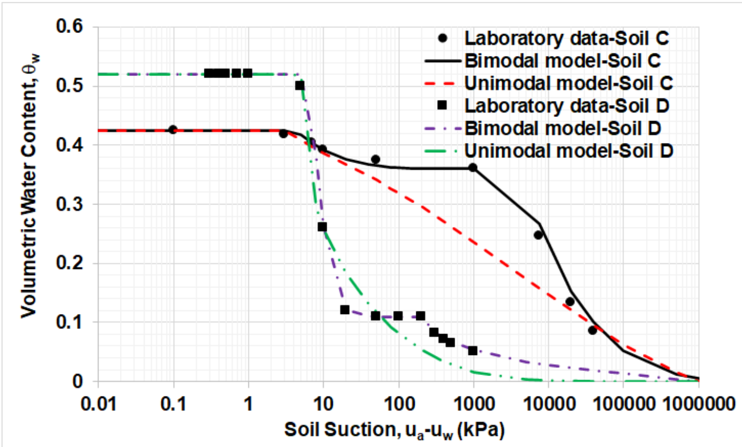

Fig. 4 Water retention curve of soils C and D modelled with dual-mode and single-mode equations

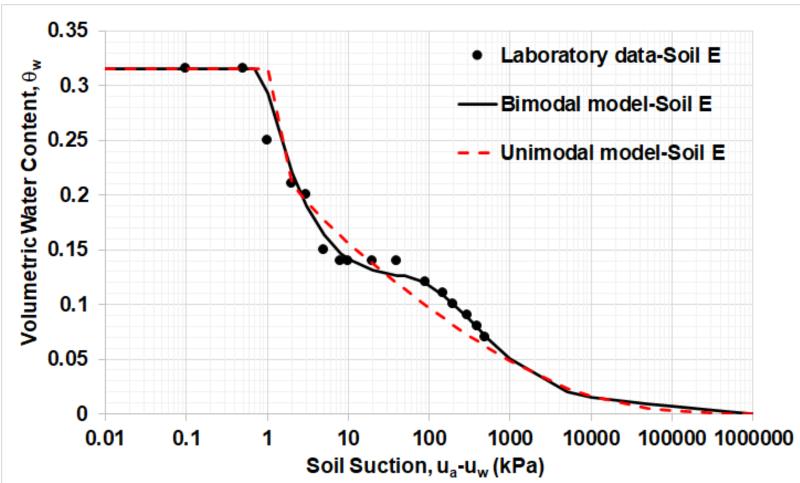

Fig. 5 Water retention curve of soil E modelled with dual-mode and single-mode equations

Statistical method was utilized to determine the unsaturated permeability of each soil in Table 3. The calculated unsaturated permeability was best fitted using the proposed equations for dual-mode (Eq. (3)) and single-mode unsaturated permeability (Eq. (4)) in this study. The slope of the unsaturated permeability from each soil in Figs. 6-8 is similar to the slope of water retention curve either for single-mode or dual-mode unsaturated permeability. In addition, the suction corresponding to the initial decrease of the permeability for each soil is closely related to the air-entry value of each soil based on Water retention curve in Figs. 3-5. It can be observed that the differences between the unsaturated permeability fitted using dual-mode and single-mode equations varied for different soil types.

Table 2 Variables of Water retention curve based on dual-mode equation

Description	Soils				
	Soil A	Soil B	Soil C	Soil D	Soil E
θ_{s1}	0.411	0.414	0.425	0.520	0.316
θ_{s2}	0.25	0.22	0.36	0.11	0.13
ψ_{a1} (kPa)	0.75	0.80	4.0	5.0	0.80
ψ_{a2} (kPa)	100	50	5000	200	50
ψ_{m1} (kPa)	8.2	3.0	10	9.0	2.0
ψ_{m2} (kPa)	5000	500	15000	400	500
s_1	1.2	0.9	1.5	0.7	1.5
s_2	2.0	1.5	2.1	2.0	1.5
θ_r (kPa)	0.03	0.00	0.00	0.04	0.02
ψ_r (kPa)	20000	5000	10000	1000	1000
$RMSE_b$	0.006	0.009	0.012	0.005	0.013
ARE_b	1.7	2.9	2.1	1.5	4.2

Table 3 Variables of Water retention curve based on single-mode equation

Description	Soils				
	Soil A	Soil B	Soil C	Soil D	Soil E
θ_s	0.411	0.414	0.425	0.520	0.316
ψ_a (kPa)	1.5	1.0	4.0	5.0	1.0
ψ_m (kPa)	184	10	1000	10	9.5
s	4.0	2.0	4.0	3	5.0
ψ_r (kPa)	1000	100	50000	300	1000
θ_r (kPa)	0.10	0.13	0.05	0.00	0.00
$RMSE_u$	0.015	0.032	0.034	0.030	0.023
ARE_u	4.9	11.5	8.7	24	12

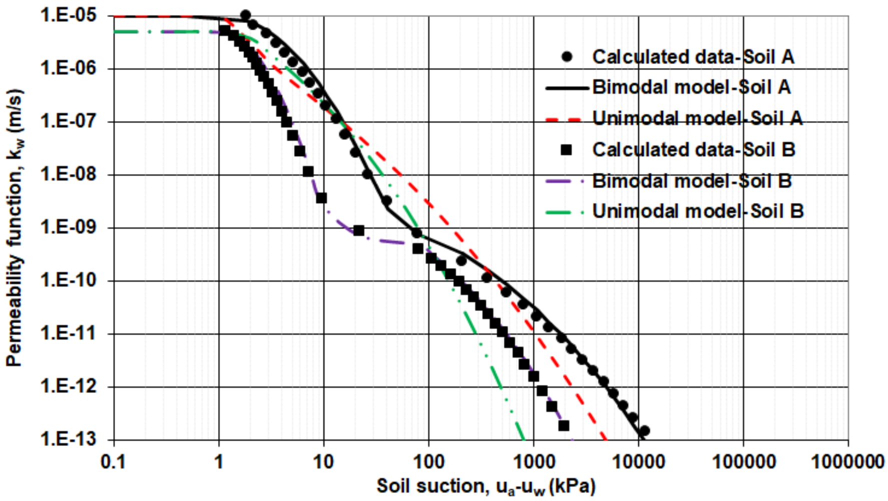

Fig. 6 The unsaturated permeability of the investigated soils A and B best fitted using single-mode and dual-mode equations

4. Finite element analyses

The influence of the partially saturated properties of dual-porosity soils on the slope stability during rainfall was investigated using transient seepage analyses and limit equilibrium slope stability analyses. Seep/W (Satyanaga and Rahardjo 2019) was utilized to carry out finite element seepage analyses. Slope/W (Satyanaga and Rahardjo 2019) was utilized to conduct slope stability analyses. The highest cumulation of rainfall for 1 day for design of drainage

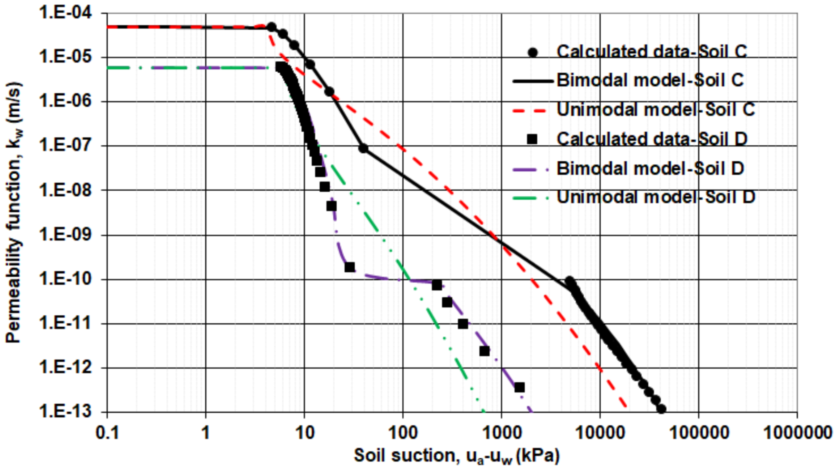

Fig. 7 The unsaturated permeability of the investigated soils C and D best fitted using single-mode and dual-mode equations

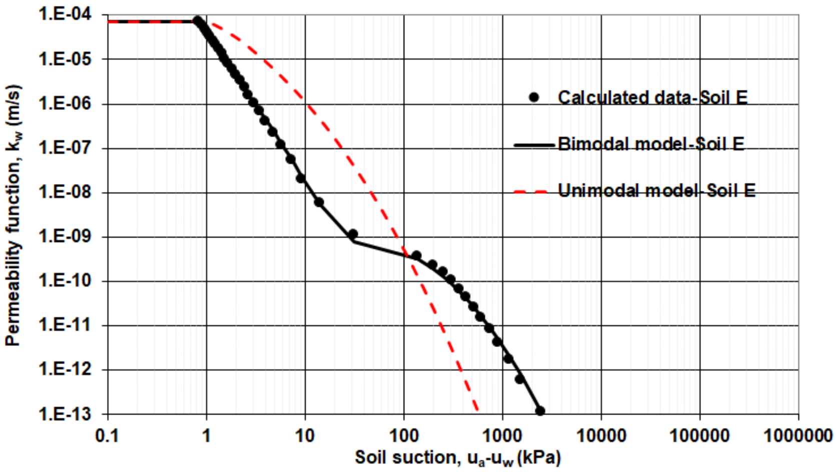

Fig. 8 The unsaturated permeability of the investigated soils E best fitted using single-mode and dual-mode equations

system in Singapore (Public Utilities Board 2000) was applied as flux boundary condition in the seepage analyses. The maximum rainfall intensity of 22 mm/h for 1 day was incorporated as downward loading within the slope surface in the analyses. The same flux boundary condition was applied for analyses of different type of soils presented in Tables 2 and 3.

Five sets of numerical analyses were performed in this study. Each set consists of two cases of finite element seepage and slope stability analyses conducted on each dual porosity soil presented in Table 1. All slope models were simulated using the same slope geometry and groundwater table location. The differences are in the soil properties which were taken from soils A to E in Table 1. The soil profile for all sets is assumed homogeneous. In Case 1, the water retention curve was modelled using the dual-mode equation (Eq. (1) from Satyanaga *et al.* 2013). The unsaturated permeability in Case 1 was modelled using Eq. (2) proposed in this study. In Case 2, the water retention curve was modelled using the single-mode equation (Satyanaga *et al.* 2017 equation). The unsaturated permeability in Case 2 was modelled using Eq. (3) proposed in this study.

The initial pore-water pressures were assumed hydrostatic for all sets of numerical analyses. In other words, the initial condition used in the seepage analysis was based on the groundwater table condition. The zero pore-water pressures at the groundwater table position. This pore-water pressure decreases into the maximum value of negative pore-water pressure at the ground surface. Fig. 9 presents the numerical model and the boundary condition used in all analyses. The slope model in all cases of the analyses had 15 m height and 27 degree inclination. The groundwater table was located 1 m depth below the toe of the slope and 6 m depth below the crest of the slope. The geometry of the slope and the initial condition of groundwater table were determined based on typical geometry and groundwater table position for residual soil slopes in Singapore (Chan *et al.* 2020).

Morgenstern-Price method was utilized in the limit equilibrium analyses to determine the stability of dual porosity soil slopes under dry and rainy periods. The pore-water pressures variations with time from finite element seepage analyses were extracted from Seep/W and exported to Slope/W for slope stability analyses. Table 4 presents the saturated and partially saturated soil properties used in the

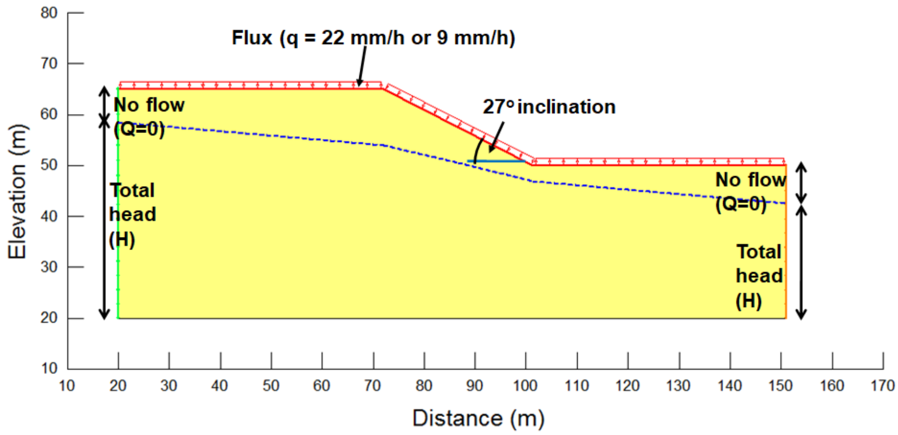

Fig. 9 Numerical model of all slopes in transient seepage analyses

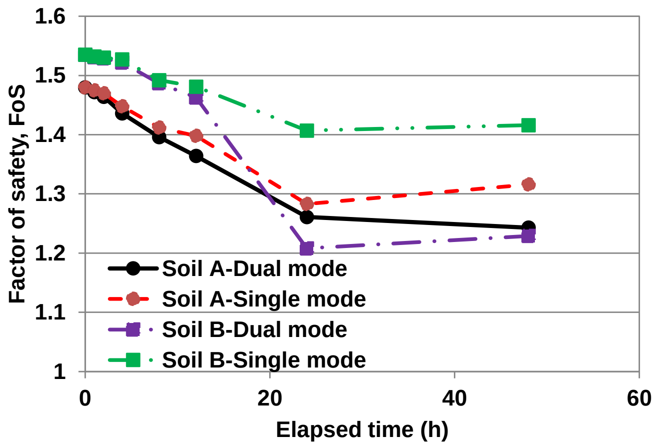

Fig. 10 Variations in safety factor for soils A and B modeled with (a) dual-mode and (b) single-mode equations

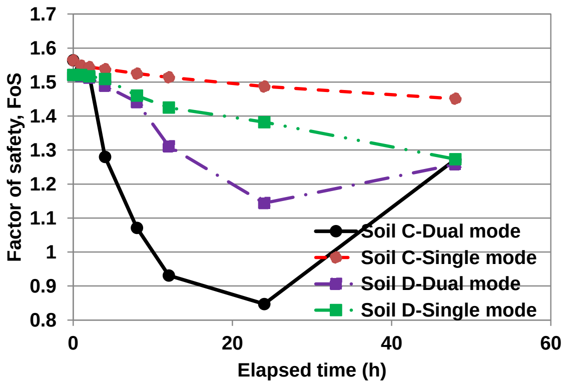

Fig. 11 Variations in safety factor for soils C and D modeled with (a) dual-mode and (b) single-mode equations

analyses for determination of variations in safety factor in Slope/W. The results from stability analyses are presented in Figs. 10-12.

The results from slope stability analyses (Figs. 10-12) indicated that the differences between the initial and the minimum safety factor for dual porosity soil slope C are the largest as compared to other slopes. This might be attributed to the higher permeability of soil 3 than other soils within partially saturated condition. As a result, the rainwater percolated down faster into a deeper soil layer during heavy rainfall in comparison with soil layers within slope A, B, D and E. The stability analysis results also showed that safety factor during the application of rainfall for slope with soils modelled with single-mode equation were higher as compared to those modelled with dual-mode equation. This might occur since the unsaturated permeability for slope with soils modelled with single-mode equation were higher as compared to those modelled with dual-mode equations. As a result, it is easier for the rainwater to be drained out into the toe of the slope for soils with single-mode equation

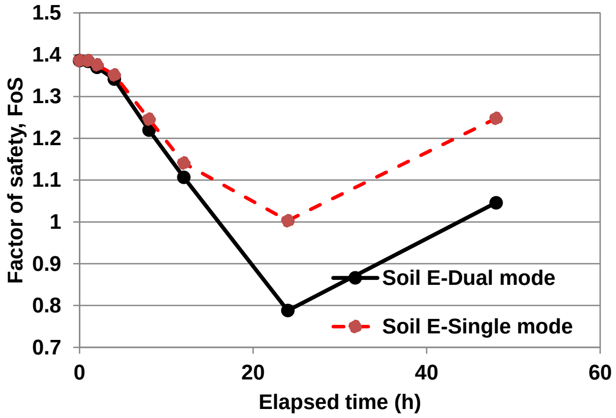

Fig. 12 Variations in safety factor for soil E modeled with (a) dual-mode and (b) single-mode equations

Table 4 Shear strength of soils A to E

Description	Soils				
	Soil A	Soil B	Soil C	Soil D	Soil E
Effective cohesion, c' (kPa)	10	2	0	0	1
Effective friction angle, ϕ' (°)	26	32	29	33	30
Unsaturated shear strength angle, ϕ_b (°)	16	19	15	22	28

as compared to those modelled with dual-mode equation. The slower rate of water flow within the soils with dual-mode equation may cause the perched water table within the soil layer that attributed to the lower factor of safety for the soils modelled with dual-mode equation as compared to those modelled with single-mode equation.

It can be observed from Tables 2 and 3 as well as Figs. 10-12 that the soil with the highest AREu of its water retention curve among all soils is associated with the largest percentage of difference in the safety factor variations. As opposed, soils with the lowest AREu of its water retention curve among all soils is associated with the lowest percentage of difference in the safety factor variations. The results from this study showed that the analyses of slope incorporating soils modelled with dual-mode water retention curve and dual-mode unsaturated permeability are associated with more conservative results of stability analyses. The stability analyses indicated that it is important to model the dual porosity soils using dual-mode water retention curve and dual-mode unsaturated permeability. The modelling of dual porosity soils using single-mode water retention curve and single-mode unsaturated permeability would result in the higher safety factor of the soil slope.

5. Conclusions

The new equations for modelling single-mode and dual-mode unsaturated permeability have been developed in this study. The water retention curve of dual porosity soils were modelled using the published single-mode and dual-mode equations. The unsaturated permeability of dual porosity soils were modelled using the proposed single-mode and dual-mode equations. The findings from the stability analyses of dual porosity soils indicated that the decreases in safety factor for slope with soils fitted using single-mode equation is lower as compared to those fitted using dual-mode equation. The largest percentage of differences between soils fitted with single-mode and dual-mode equations were observed within the minimum safety factor. The minimum safety factor for slope with soils fitted using dual-mode equation is much lower as compared to those fitted using single-mode equation. In conclusion, the water retention curve and the unsaturated permeability of dual porosity soils should be modelled using the dual-mode equation to obtain reasonable factor of safety of the slope.

Acknowledgments

This research was supported by the Nazarbayev University Research Fund under Grants #SOE2017003. The authors are grateful for this support. Any opinions, findings, and conclusions or recommendations expressed in this material are those of the author(s) and do not necessarily reflect the views of the Nazarbayev University.

References

Al-Mahbashi, A.M., Elkady, T.Y. and Alrefeai, T.O. (2015), "Soil water characteristic curve and improvement in lime treated expansive soil", *Geomech. Eng.*, **8**(5), 687-696. https://doi.org/10.12989/gae.2015.8.5.687.

ASTM D2487-17e1 (2017), Standard Practice for Classification of Soils for Engineering Purposes (Unified Soil Classification System). American Society for Testing and Materials; ASTM International, Pennsylvania, USA.

Brooks, R.H. and Corey, A.T. (1964), *Hydraulic Properties of Porous Media*, Fort Collins: Colorado State University, Colorado, USA.
Burger, C.A. and Shackelford, C.D. (2001), "Evaluating dual porosity of pelletized diatomaceous earth using bimodal soil-water characteristic curve functions", *Can. Geotech. J.*, **38**(1), 53-66. https://doi.org/10.1139/t00-084.
Chan, Y.E.C., Ng, Q.L., Satyanaga, A. and Rahardjo, H. (2020), "Regional stability and adaptation measures against rainfall-induced slope failures", *Environ. Geotechnics*, Published online on 29 January 2021, 1-16. https://doi.org/10.1680/jenge.20.00089.
Childs, E.C. and Collis-George, N. (1950), "The permeability of porous materials", *Proceedings of The Royal Society A*, **201**(1066), 392-405. https://doi.org/10.1098/rspa.1950.0068.
Coutinho, R.Q., Silva, M.M. and Lafayete, K. (2011), "Geotechnical characterization of two unsaturated mature granite residual soils from Pernambuco, Brazil", *Proceedings of 14th Pan-American Conference on Soil Mechanics and Geotechnical Engineering 64th Canadian Geotechnical Conference*, Toronto, Canada, October.
Deng, D., Wen, S., Lu, K. and Li, L. (2020), "Calculation model for the shear strength of unsaturated soil under nonlinear strength theory", *Geomech. Eng.*, **21**(3), 247-258. http://dx.doi.org/10.12989/gae.2020.21.3.247.
Deng, D., Lu, K. and Li, L. (2019), "LE analysis on unsaturated slope stability with introduction of nonlinearity of soil strength", *Geomech. Eng.*, **19**(2), 179-191. https://doi.org/10.12989/gae.2019.19.2.179.
Durner, W. (1994), "Hydraulic conductivity estimation for soil with heterogeneous pore structure", *Water Resour. Res.*, **30**(2), 211-223. https://doi.org/10.1029/93WR02676.
Fredlund, D.G. and Xing, A. (1994), "Equations for the soil-water characteristic curve", *Can. Geotech. J.*, **31**(3), 521-532. https://doi.org/10.1139/t94-061.
Fredlund, D.G. and Rahardjo, H. (1993), *Soil Mechanics for Unsaturated Soils*, John Wiley & Sons, Inc., New York, NY, USA.
Fredlund, D.G., Rahardjo, H. and Fredlund, M.D. (2012), *Unsaturated Soil Mechanics in Engineering Practice*, John Wiley & Sons, Inc., New York, NY, USA.
Fredlund, M.D., Wilson, G.W. and Fredlund, D.G. (2002), "Use of the grain-size distribution for estimation of the soil-water characteristic curve", *Can. Geotech. J.*, **39**(5), 1103-1117. https://doi.org/10.1139/t02-049.
Fredlund, D.G., Xing, A. and Huang, S. (1994), "Predicting the permeability function for unsaturated soils using the soil-water characteristic curve", *Can. Geotech. J.*, **31**(4), 533-546. https://doi.org/10.1139/t94-062.
Gardner, W.R (1958), "Mathematics of isothermal water conduction in unsaturated soils", *Proceedings of the 37th Annual Meeting of the Highway Research Board*, Washington D.C., USA, January.
Gitirana Jr., G.F.N. and Fredlund, D.G. (2004), "Soil-water characteristic curve equation with independent properties", *J. Geotech. Geoenviron. Eng.*, **130**(2), 209-212. https://doi.org/10.1061/(ASCE)1090-0241(2004)130:2(209).
Delleur, J.W. (1999), *Handbook of Groundwater Engineering*, CRC Press, New York, NY, USA.
Jotisankasa, A., Vathananukij, H. and Coop, M.R. (2009), "Soil-water retention curves of some silty soils and their relations to fabrics", *Proceedings of The 4th Asia Pacific Conference on Unsaturated Soils*, Newcastle, Australia, November.
Jotisankasa, A. and Mairaing, W. (2010), "Suction-monitored direct shear testing of residual soils from landslide-prone areas", *J. Geotech. Geoenviron. Eng.*, **136**(3), 533-537. https://doi.org/10.1061/(ASCE)GT.1943-5606.0000225.
Kassim, A., Lee, M.L., Gofar, N. and Rahardjo, H. (2012), "Modelling of suction distributions in an unsaturated heterogeneous residual soil slope", *J. Eng. Geology*, **131-132**, 70-82. https://doi.org/10.1016/j.enggeo.2012.02.005.
Kim, Y. and Jeong, S. (2017), "Modeling of shallow landslides in an unsaturated soil slope using a coupled model", *Geomech. Eng.*, **13**(2), 353-370. https://doi.org/10.12989/gae.2017.13.2.353.
Kosugi, K. (1994), "Lognormal distribution model for unsaturated soil hydraulic properties", *Water Resour. Res.*, **32**(9), 2697-2703. https://doi.org/10.1029/96WR01776.
Krisnanto, S., Rahardjo, H. and Leong, E.C. (2020), "Numerical study on the effect of crack network representation on water content in cracked soil", *Geomech. Eng.*, **21**(6), 537-549. https://doi.org/10.12989/gae.2020.21.6.537.
Kristo, C., Rahardjo, H. and Satyanaga, A. (2019), "Effect of hysteresis on the stability of residual soil slope", *Int. Soil Water Conservation Res.*, **7**(3), 226-238. https://doi.org/10.1016/j.iswcr.2019.05.003.
Kunze, R.J., Uehara, G. and Graham, K. (1968), "Factors important in the calculation of hydraulic conductivity", *Soil Sci. Soc. Am. J.*, **32**(6), 760-765. https://doi.org/10.2136/sssaj1968.03615995003200060020x.
Li, X., Li, J.H. and Zhang, L.M. (2014), "Predicting bimodal soil-water characteristic curves and permeability functions using physically based parameters", *Comput. Geotech.*, **57**, 85-96. https://doi.org/10.1016/j.compgeo.2014.01.004.
Leong, E.C. and Rahardjo, H. (1997), "Review of soil-water characteristic curve equations", *J. Geotech. Geoenviron. Eng.*, **123**(12), 1106-1117. https://doi.org/10.1061/(ASCE)1090-0241(1997)123:12(1106).
Mallants, D., Tseng, P.H., Toride, N., Tinunerman, A. and Feyen, J. (1997), "Evaluation of multimodal hydraulic functions in characterizing a heterogeneous field soil", *J. Hydrology*, **195** (1-4), 172-199. https://doi.org/10.1016/S0022-1694(96)03251-9.
Mustafa, M.R., Rezaur, R.B., Rahardjo, H., Isa, M.H. and Arif, A. (2015), "Artificial neural network modeling for spatial and temporal variations of pore-water pressure responses to rainfall", *Adv. Meteorology*, **2015**(273730), 1-12. https://doi.org/10.1155/2015/273730.
Othmer, H., Diekkruger, B. and Kutilek, M., (1991), "Bimodal porosity and unsaturated hydraulic conductivity", *Soil Science*, **152**(3), 139-149. https://doi.org/10.1097/00010694-199109000-00001.
Pedroso, D.M., Sheng, D. and Zhao, J. (2009), "The concept of reference curves for constitutive modelling in soil mechanics", *Comput. Geotech.*, **36**(1-2), 149-165. https://doi.org/10.1016/j.compgeo.2008.01.009.
Public Utilities Board (2000), Code of practice on surface water drainage, Public Utilities Board, Singapore, Singapore.
Qi, S., Vanapalli, S.K., Yang, X.-G., Zhou, J.-W. and Lu, G.-D. (2019), "Stability analysis of an unsaturated expansive soil slope subjected to rainfall infiltration", *Geomechanics and Engineering*, **19**(1), 1-9. https://doi.org/10.12989/gae.2019.19.1.011.
Rahardjo, H. and Satyanaga, A. (2019) "Sensing and monitoring for assessment of rainfall-induced slope failures in residual soil", *Geotech. Eng.*, **172**(6), 496-506. https://doi.org/10.1680/jgeen.18.00208.
Rahardjo, H., Nistor, M., Gofar, N., Satyanaga, A., Qin, X. and Ip., C.Y. (2019), "Spatial distribution, variation and trend of five-day antecedent rainfall in Singapore", *Georisk: Assessment and Management of Risk for Engineered Systems and Geohazards*, **14**(3), 177-191. https://doi.org/10.1080/17499518.2019.1639196.
Rahardjo, H., Satyanaga, A., Mohamed, H., Ip, C.Y. and Shah, R.S. (2018), "Comparison of soil–water characteristic curves

from conventional testing and combination of small-scale centrifuge and dew point methods", *Geotech. Geol. Eng.*, **37**, 659-672). https://doi.org/10.1007/s10706-018-0636-2.

Rahardjo, H., Santoso, V.A., Leong, E.C., Ng, Y.S. and Tam, C.P.H. (2012), "Effect of vetiver grass on slope stability", *Proceedings of 11th International and 2nd North American Symposium on Landslides*, Banff, Canada, June.

Rahardjo, H., Santoso, V.A., Leong, E.C., Ng, Y.S. and Hua, C.J. (2011), "Numerical analyses and monitoring performance of residual soil slopes", *Soils Found.*, **51**(3), 471-482. https://doi.org/10.3208/sandf.51.471.

Rahardjo, H., Meilani, I., Rezaur, R.B. and Leong, E.C. (2009), "Shear strength characteristics of a compacted soil under infiltration conditions", *Geomech. Eng.*, **1**(1), 35-52. https://doi.org/10.12989/gae.2009.1.1.035.

Rahimi, A., Rahardjo, H. and Leong, E.C. (2015), "Effect of range of soil-water characteristic curve measurements on estimation of permeability function", *Eng. Geol.*, **185**, 96-104. https://doi.org/10.1016/j.enggeo.2014.11.017.

Ross, P.J. and Smettem, K.R.J. (1993), "Describing soil hydraulic properties with sums of simple functions", *Soil Sci. Soc. Am. J.*, **57**(1), 26-29. https://doi.org/10.2136/sssaj1993.03615995005700010006x.

Satyanaga, A. and Rahardjo, H. (2019a), "Stability of unsaturated soil slopes covered with Melastoma Malabathricum in Singapore", *Proceeding of the Institution of Civil Engineers - Geotechnical Engineering*, **172**(6), 530-540. https://doi.org/10.1680/jgeen.18.00215.

Satyanaga, A. and Rahardjo, H. (2019b), "Unsaturated shear strength of soil with bimodal soil-water characteristic curve", *Géotechnique*, **69**(9), 828-832. https://doi.org/10.1680/jgeot.17.P.108.

Satyanaga, A., Rahardjo, H. and Hua, C.J. (2019), "Numerical simulation of capillary barrier system under rainfall infiltration", *ISSMGE Int. J. Geoeng. Case Histories*, **5**(1), 43-54. http://dx.doi.org/10.4417/IJGCH-05-01-04.

Satyanaga, A., Rahardjo, H. and Zhai, Q. (2017), "Estimation of unimodal water characteristic curve for gap-graded soil", *Soils Found.*, **57**(5), 789-801. https://doi.org/10.1016/j.sandf.2017.08.009.

Satyanaga, A., Rahardjo, H., Leong, E.C. and Wang, J.Y. (2013), "Water characteristic curve of soil with bimodal grain-size distribution", *Comput. Geotech.*, **48**, 51-61. https://doi.org/10.1016/j.compgeo.2012.09.008.

Sheng, D. (2011), "Review of fundamental principles in modelling unsaturated soil behaviour", *Comput. Geotech.*, **38**(6), 757-776. https://doi.org/10.1016/j.compgeo.2011.05.002.

Smettem, K.R.J. and Kirkby, C., (1990), "Measuring the hydraulic properties of a stable aggregated soil", *J. Hydrology*, **117** (1-4), 1-13. https://doi.org/10.1016/0022-1694(90)90084-B.

Van Genuchten, M.T. (1980), "A close form equation predicting the hydraulic conductivity of unsaturated soil", *Soil Sci. Soc. Am. J.*, **44**(5), 892-898. https://doi.org/10.2136/sssaj1980.03615995004400050002x.

Wijaya, M. and Leong, E.C. (2016), "Equation for unimodal and bimodal soil–water characteristic curves", *Soils Found.*, **56**(2), 291-300. https://doi.org/10.1016/j.sandf.2016.02.011.

Wilson, G.V., Jardine, P.M. and Gwo, J.P. (1992), "Modeling the hydraulic properties of a multi-region soil", *Soil Sci. Soc. Am. J.*, **56**(6), 1731-1737. https://doi.org/10.2136/sssaj1992.03615995005600060012x.

Zhai, Q., Rahardjo, H., Satyanaga, A., Dai, G and Zhuang, Y (2020), "Framework to estimate the soil-water characteristic curve for soils with different void ratios", *Bull. Eng. Geology Environ.*, **79**, 4399-4409. https://doi.org/10.1007/s10064-020-01825-8.

Zhai, Q., Rahardjo, H. and Satyanaga, A. (2018), "A pore-size distribution function based method for estimation of hydraulic properties of sandy soils", *Eng. Geol.*, **246**, 288-292. https://doi.org/10.1016/j.enggeo.2018.09.031

Zhai, Q., Rahardjo, H., Satyanaga, A. and Priono (2017), "Effect of bimodal soil-water characteristic curve on the estimation of permeability function", *Eng. Geol.*, **230**(9), 142-151. https://doi.org/10.1016/j.enggeo.2017.09.025.

Zhai, Q., Rahardjo, H. and Satyanaga, A. (2017), "Effects of residual suction and residual water content on the estimation of permeability function", *Geoderma*, **303**(1), 165-177. https://doi.org/10.1016/j.geoderma.2017.05.019.

Zhai, Q. and Rahardjo, H. (2015), "Estimation of permeability function from the soil-water characteristic curve", *Eng. Geol.*, **199**, 148-156. https://doi.org/10.1016/j.enggeo.2015.11.001.

Zhang, L. and Chen, Q. (2005), "Predicting bimodal soil-water characteristic curves", *J. Geotech. Geoenviron. Eng.*, **131**(5), 666-670. https://doi.org/10.1061/(ASCE)1090-0241(2005)131:5(666).

IC